Optimal Frequency Reuse for Regular Multibeam Satellite Antennas

Francesco Lisi*†, Piero Angeletti‡, João F. C. Mota†, Julien Maurin*, Hervé Legay*, George Goussetis†
*Thales Alenia Space, Toulouse, France, {francesco.lisi, julien.maurin, herve.legay}@thalesaleniaspace.com
†Heriot-Watt University, Edinburgh, UK, {f.lisi, j.mota, g.goussetis}@hw.ac.uk
‡European Space Agency, Noordwijk, the Netherlands, piero.angeletti@esa.int

***Abstract*—This paper addresses optimal frequency reuse in multibeam satellite systems featuring regular beam lattices, such as those employed in GEO, MEO, and LEO constellations. To maximize spectral efficiency while mitigating co-channel interference, the study formulates the resource assignment problem as an optimization over lattice substructures. We apply the maximum same-colour nearest-neighbour sublattice (MASCONDS) algorithm, a globally optimal method that identifies the sublattice partition maximizing the minimum co-channel distance for any lattice and reuse factor. Numerical analyses with a hexagonal lattice for a non-canonical reuse factor validate the approach using a GEO communication payload with a direct radiating array model operating in Ka-band. The MASCONDS solution consistently yields the highest carrier-to-interference ratio across all configurations. These results demonstrate the method's effectiveness for advanced satellite payloads constrained by digital processor port counts.**

***Index Terms*—Radio resource assignment, frequency reuse, wireless communications, satellite communications, lattice theory.**

I. Introduction

In modern high-throughput satellite communication systems, including those deployed in geostationary (GEO), medium (MEO), and low (LEO) Earth orbit, the imperative to maximize data capacity calls for the use of aggressive frequency reuse. Large service regions are covered by a periodic grid of spot beams, often idealized as a *multibeam lattice*. The available frequency spectrum, or any other orthogonal radio resource (collectively referred to as a 'colour'), is reused across different beams to boost overall system capacity. This practice, however, comes at the cost of high Co-Channel Interference (CCI), which is a dominant limiting factor on the achievable Spectral Efficiency (SE). Mitigating CCI through careful planning is thus essential for system performance.

Many advanced satellite architectures [1-2], even those featuring digital payloads [3], employ a fixed, regular beam lattice due to practical constraints related to payload complexity and antenna implementation [4-5]. Consequently, the resource assignment must rely on a static geometric partitioning. This is achieved by segmenting the primary beam lattice into a set of periodic *sublattices*, where all beams belonging to the same sublattice are assigned the same colour. As an example, Fig.1a and Fig.1b show two ways of partitioning a hexagonal lattice into sublattices with 3 colours. The quality of this geometric scheme determines the level of interference experienced by users. The core technical problem is therefore one of discrete geometry: *to select the optimal sublattice configuration that maximizes the minimum distance between any two co-channel beams*, thereby minimizing CCI and maximizing SE.

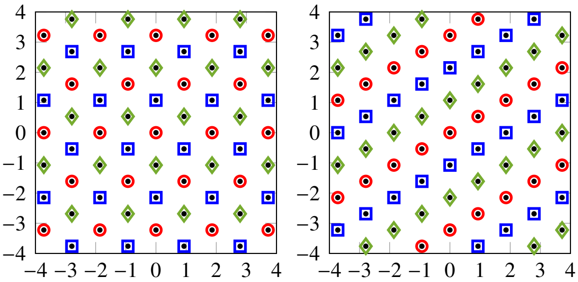

(a) Config. A (b) Config. B

Figure 1: Plot of two different sublattices of a hexagonal lattice with 3 colours.

Existing analytical methods often rely on number theory, particularly Diophantine equations, which were developed decades ago to address specific lattice types (e.g., hexagonal or square) [6-7]. While historically significant, these approaches suffer from two major limitations. First, they only yield integer solutions for a restricted subset of possible reuse factors, C. Second, for certain lattices (like the square lattice), the solutions derived are known to be sub-optimal, failing to guarantee the maximum possible co-channel separation. Thus, for an arbitrary, non-canonical number of resources C and a general two-dimensional lattice (which are becoming of practical interest [4]), system designers lacked a rigorous method to guarantee the highest performing geometric layout. Therefore, in [8], we introduced the maximum same-colour nearest-neighbour sublattice (MASCONDS) algorithm, that provides a universal, globally optimal solution procedure for resource assignment. The work provides a unified, constructive solution by addressing a core geometric question applicable to modern multibeam systems:

Given a regular beam lattice and an arbitrary number of colours C, what is the partition into regular sublattices that ***maximizes the minimum co-channel distance*** *($d_{\min}$), consequently minimizing interference?*

After reporting the main results in [8], in this manuscript we compare the carrier-to-interference ratio (C/I) performance of a GEO multibeam satellite operating in Ka band considering all possible sublattices of a hexagonal lattice with a non canonical number of colours $C = 80$. Contrary to the example

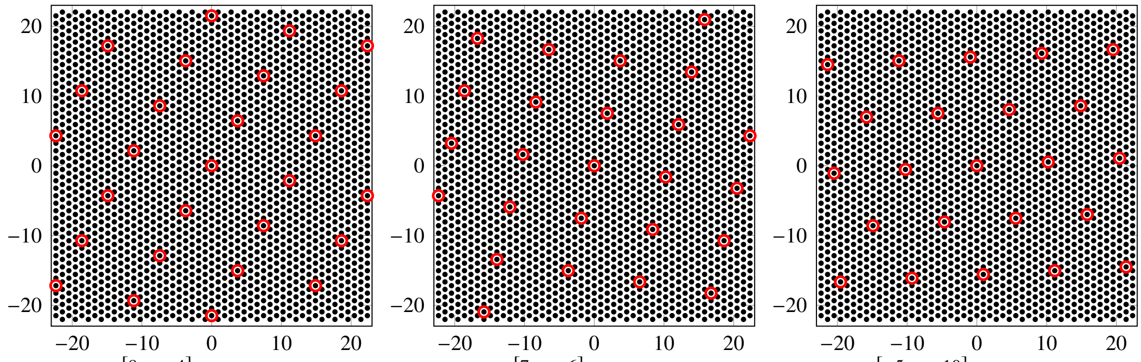

(a) $\boldsymbol{M} = \begin{bmatrix} 8 & -4 \\ 4 & 8 \end{bmatrix}$, $d_{\min} = 4\sqrt{2}\sqrt[4]{3} \simeq 7.44$. (b) $\boldsymbol{M} = \begin{bmatrix} 7 & -6 \\ 4 & 8 \end{bmatrix}$, $d_{\min} = \frac{2\sqrt{2\cdot 13}}{\sqrt[4]{3}} \simeq 7.75$ (c) $\boldsymbol{M} = \begin{bmatrix} -5 & -10 \\ 10 & 4 \end{bmatrix}$, $d_{\min} = 5\sqrt{2}\sqrt[4]{3} \simeq 9.31$.

Figure 2: Plot of three sublattices of a hexagonal lattice (with $\det \boldsymbol{D} = 1$) with $C = 80$ colours. The red marks denote the sublattice elements associated to the colour that includes the element in the origin. (a) and (b) are randomly selected solutions, (c) is the optimal solution obtained with the MASCONDS algorithm, which provides the largest $d_{\min}$ among all solutions.

in [8], in this manuscript we validate our approach with a more realistic antenna model, i.e. a direct radiating array (DRA) with a limited number of radiating elements in line with the constraint on the number of ports that can be connected to a state-of-the-art digital transparent processor (DTP) [3]. The numerical results confirm that the solution obtained with the MASCONDS algorithm provides the best C/I performance among all possible sublattices.

II. Lattice Theory and Problem Formulation

A high-throughput multibeam satellite system uses a periodic arrangement of spot beams, which can be modelled mathematically as a uniform lattice $\Lambda(\boldsymbol{D})$ in $\mathbb{R}^2$ [5], [9]. The lattice is defined by a non-singular basis matrix,

$$\boldsymbol{D} = [\boldsymbol{d}_1, \boldsymbol{d}_2] \in \mathbb{R}^{2\times 2} \tag{1}$$

such that its points are

$$\boldsymbol{r} = \boldsymbol{D}\boldsymbol{n}\ , \text{with} \ \ \boldsymbol{n} \in \mathbb{Z}^2 \tag{2}$$

We assume $\boldsymbol{D}$ is in *reduced form*, corresponding to the shortest vector lattice basis [8].

Frequency reuse is achieved by partitioning the primary lattice $\Lambda(\boldsymbol{D})$ into C distinct sublattices. Each sublattice corresponds to the set of points assigned the same resource (colour). A single sublattice Λ' is mathematically generated by a transformation of the original basis:

$$\Lambda' = \Lambda(\boldsymbol{D}\boldsymbol{M}), \tag{3}$$

where $\boldsymbol{M} \in \mathbb{Z}^{2\times 2}$ is an integer matrix. The reuse factor C is determined by the determinant of this matrix,

$$C = |\det \boldsymbol{M}|\ . \tag{4}$$

The objective is to mitigate CCI by maximizing the distance between co-channel beams. This is equivalent to finding the transformation matrix $\boldsymbol{M}_C^\star$ that yields the maximum possible minimum distance ($d_{\min}$) between any two points in the same sublattice:

$$\boldsymbol{M}_C^\star \in \underset{\substack{\boldsymbol{M}\in\mathbb{Z}^{2\times 2} \\ |\det \boldsymbol{M}|=C}}{\arg\max} \ \min_{\boldsymbol{n}\in\mathbb{Z}^2\setminus\{\boldsymbol{0}\}} \|\boldsymbol{D}\boldsymbol{M}\boldsymbol{n}\|\,. \tag{5}$$

The optimal matrix $\boldsymbol{M}_C^\star$ is key to ensuring maximum SE for the system.

III. MASCONDS Algorithm

The critical challenge in solving (5) is that multiple transformation matrices $\boldsymbol{M}$ can generate the same sublattice, leading to computational redundancy. To ensure a non-redundant and globally optimal search, the MASCONDS algorithm leverages the *Hermite Normal-Form (HNF) theorem*.

Every unique sublattice Λ' is represented by one and only one non-singular integer matrix $\boldsymbol{H}$ in HNF, satisfying two properties:

- it is upper triangular, and
- its off-diagonal elements are non-negative and smaller than the pivot elements.

This allows us to restrict the search space from all possible $\boldsymbol{M}$ matrices to the finite set $\mathcal{H}_{2,C}$ of HNF matrices with $|\det \boldsymbol{H}| = C$. The problem is thus reformulated as:

$$\boldsymbol{H}_C^\star \in \arg \max_{\boldsymbol{H}\in\mathcal{H}_{2,C}} \ \min_{\boldsymbol{n}\in\mathbb{Z}^2\setminus\{\boldsymbol{0}\}} \|\boldsymbol{D}\boldsymbol{H}\boldsymbol{n}\|\,. \tag{6}$$

The MASCONDS algorithm solves (6) via a complete, non-redundant enumeration as follows [8]:

1) **Generation:** All possible HNF matrices $\boldsymbol{H} \in \mathcal{H}_{2,C}$ are generated based on the prime factorization of C.
2) **Sublattice Basis:** For each candidate $\boldsymbol{H}$, the candidate sublattice basis matrix is calculated as $\boldsymbol{V} = \boldsymbol{D}\boldsymbol{H}$.
3) **Distance Calculation:** An exact Lattice Reduction Algorithm (e.g., the Lagrange algorithm for $N = 2$ [10]) is applied to $\boldsymbol{V}$. The shortest vector found (the first column of the reduced $\boldsymbol{V}$) corresponds directly to the minimum co-channel distance $d_{\min}$ for that configuration.
4) **Optimization:** The algorithm selects the HNF matrix $\boldsymbol{H}^\star$ that produced the maximum value of $d_{\min}$.

Due to the non-redundant nature of the HNF set, this procedure is guaranteed to find the *globally optimal solution*. Furthermore, the per-candidate calculations are independent, allowing for efficient parallelization.

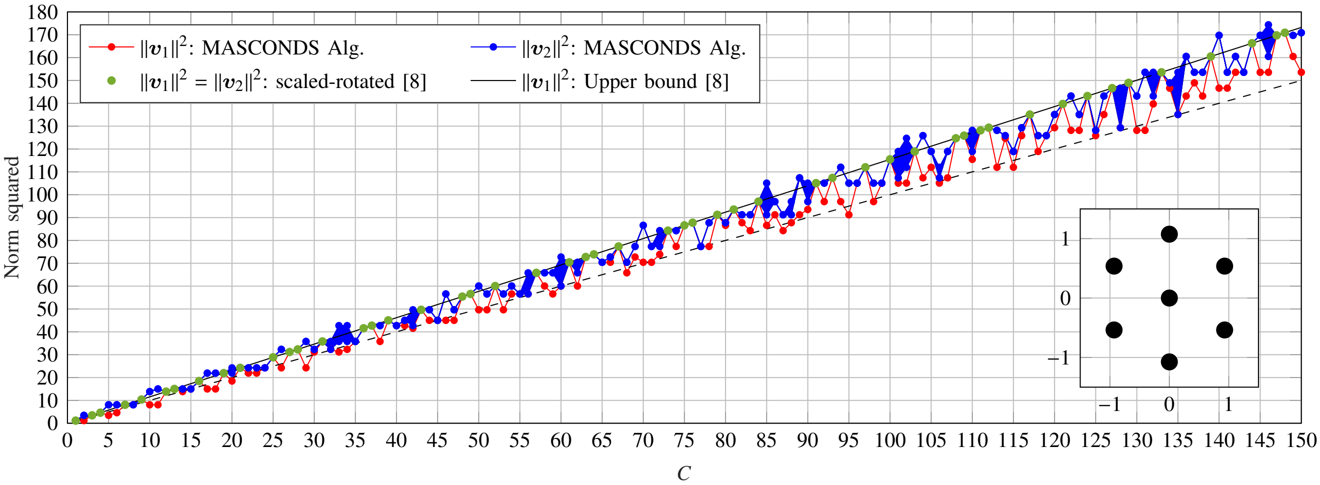

Figure 3: Plot of the squared norm of the first and second shortest sublattice vectors as a function of the numbers of colours C for a hexagonal lattice. $\boldsymbol{V} = [\boldsymbol{v}_1, \boldsymbol{v}_2]$ is the reduced sublattice matrix. The red and blue curves are obtained using the MASCONDS Algorithm. Since multiple lattices with different $\|\boldsymbol{v}_2\|$ can achieve the same $\|\boldsymbol{v}_1\|$, the blue region is the one subtended between the minimum and maximum values. The green dots correspond to the scaled-rotated sublattice ($\|\boldsymbol{v}_2\|^2 = \|\boldsymbol{v}_1\|^2$). The solid black line corresponds to the upper bound in [8].

IV. Numerical Results

Fig.2 shows an example of a partitioning of a hexagonal lattice into $C = 80$ sublattices. We purposely chose $C = 80$, as this is not a canonical colour for the hexagonal lattice, i.e. it does not satisfy the Diophantine equation in [6]. Fig.2a and Fig.2b are two randomly selected examples of sublattices, while Fig.2c is obtained by running the MASCONDS algorithm. Given its global optimality, the MASCONDS solution provides the largest $d_{\min}$ among the three solutions with a value of 9.31 against 7.44 and 7.75 for the sublattices in Fig.2a and Fig.2b, respectively.

Fig.3 shows how $d^2_{\min}$ changes with the number of colours C for a hexagonal lattice with $\det \boldsymbol{D} = 1$. The red dots in the figure represent $d^2_{\min} = \|\boldsymbol{v}_1\|^2$ for the MASCONDS solution, while the blue dots represent the norm of the second shortest vector in the sublattice $\|\boldsymbol{v}_2\|^2$. Since multiple sublattices can achieve the same $d_{\min}$, but have different $\|\boldsymbol{v}_2\|$, the blue region in the plot subtends the minimum and maximum $\|\boldsymbol{v}_2\|$ values. For the canonical C values, the MASCONDS solution corresponds to the scaled-rotate sublattice [8], which is a hexagonal sublattice itself. This is not a surprising result since the hexagonal lattice is the one that achieves the largest spacing among all planar lattices with the same density. Therefore, the scaled-rotated solution corresponds to the optimal solution for the hexagonal lattice case and regularly achieves the upper bound in [8].

A. GEO Communication Performance Example

In this section we apply the MASCONDS algorithm to identify the beam layout in a multibeam GEO communication satellite operating in Ka band. The performance is evaluated at 19.5 GHz.

The beams are uniformly arranged on a hexagonal lattice over a circular coverage of radius 4°. Each beam is assigned to one of the $C = 80$ available colours by applying the sublattice strategy described in the previous sections. The inter-beam spacing in the u-v plane is chosen in such a way that the distance between the two closest neighbouring beams assigned to the same resource is equal to the antenna's half power beamwidth (HPBW) for the MASCONDS solution.

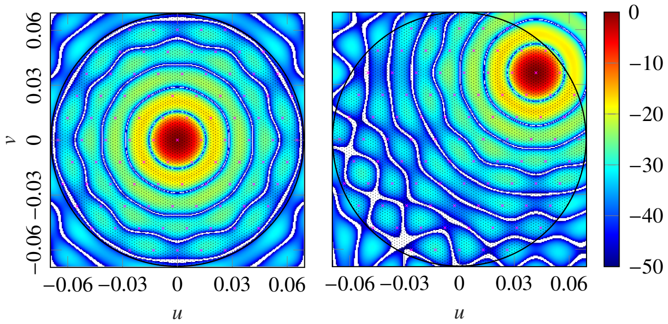

(a) Beam at (0,0). (b) Beam at $(3.75,3.90)10^{-2}$.

Figure 4: Normalised radiation pattern (dB) of the central and a scanned beam. The white crosses correspond to the beam centres for colour 1 considering the largest nearest-neighbour distance sublattice. The black crosses correspond to the beam centres of all the remaining colours.

The antenna corresponds to a circular DRA of diameter $D = 1.2$ m with elements arranged in a hexagonal lattice with inter-element spacing

$$\delta = \frac{2}{\sqrt{3}} \frac{\lambda}{\sin 4^\circ + \sin 8.7^\circ} \simeq 5.2\lambda, \tag{7}$$

which guarantees that all grating lobes' centres are outside Earth for all scan angles. Such a large inter-element spacing is necessary to connect all 199 radiating elements to the DTP, in line with the number of ports supported by state-of-the-art DTPs [3].

Each element radiates an ideal right-hand circularly polarised $\cos^q \theta$ pattern over the upper hemisphere only. The

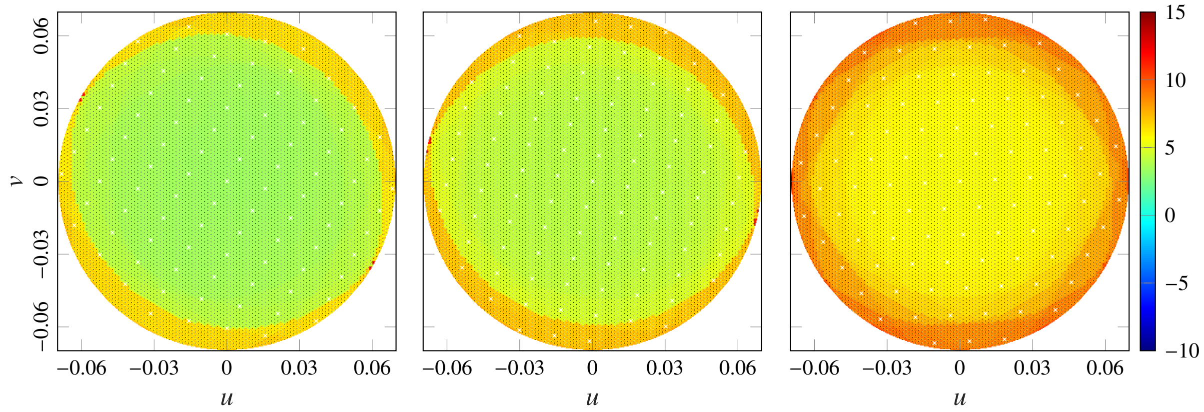

(a) $M = \begin{bmatrix} 8 & -4 \\ 4 & 8 \end{bmatrix}$. (b) $M = \begin{bmatrix} 7 & -6 \\ 4 & 8 \end{bmatrix}$. (c) $M = \begin{bmatrix} -5 & -10 \\ 10 & 4 \end{bmatrix}$, MASCONDS.

Figure 5: Surface plot of the C/I for the three sublattices with $C = 80$ in Fig.1. The plot is obtained by considering all beams simultaneously active and by assigning the user to the closest beam. The white crosses correspond to the beams' centres for colour 1, while the small black crosses to the ones of all remaining colours.

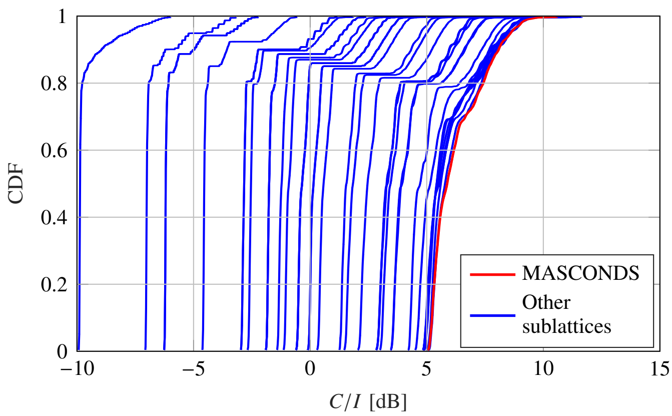

Figure 6: CDF of the C/I for all sublattices with $C = 80$ of an hexagonal lattice. The red curve represents the MASCONDS solution. The blue curves represent all the other sublattices.

q value is obtained from the element's directivity as $q = D_e/4 - 1/2$ [5], and

$$D_e = \eta \frac{4\pi}{\lambda^2} A_p, \tag{8}$$

where $\eta = 10^{-2/10}$ is the product of the aperture efficiency and radiation efficiency, and $A_p = 2\sqrt{3}(\delta/2)^2$ is the physical area of the hexagonal element. By considering the inter-element spacing in (7), we obtain $D_e = 22.7$ dBi, and $q = 46.3$. In reality, our ideal element will likely correspond to a smaller hexagonal array with small element spacing connected to an analog beamforming network, which leads to a hybrid beamforming DRA architecture like the one in [11].

Fig.4a and Fig.4b show the normalised beam patterns radiated by the DRA for the central beam and a steered beam, respectively. The steering is obtained by applying a linear phase shift with uniform amplitude as the excitation. The peak directivity is 45.7 and 45.1 dBi for the central and scanned beam, respectively.

The performance metric is the C/I computed as follows

$$\left[\frac{C}{I}\right]_u = \frac{\left(P_0/P^{(c_u)}_{b_u^{(c_u)}}\right)\left|E^{(c_u)}_{b_u^{(c_u)}}(r_u,\theta_u,\phi_u)\right|^2}{\sum_{b^{(c_u)}\neq b_u^{(c_u)}}\left(P_0/P^{(c_u)}_{b^{(c_u)}}\right)\left|E^{(c_u)}_{b^{(c_u)}}(r_u,\theta_u,\phi_u)\right|^2}, \tag{9}$$

where

$$E^{(c)}_{b^{(c)}}(r,\theta,\phi) = V_0 \frac{e^{-jkr}}{r}\cos^q\theta \sum_{n=1}^{N_T} e^{jk\mathbf{r}_n\cdot\left[\hat{\boldsymbol{r}}(\theta,\phi)-\hat{\boldsymbol{r}}\left(\theta^{(c)}_{b^{(c)}},\phi^{(c)}_{b^{(c)}}\right)\right]}, \tag{10}$$

where (r_u, θ_u, ϕ_u) are the spherical coordinates of user u in the satellite coordinate system, c_u and $b_u^{(c_u)}$ are the colour and beam assigned to user u based on the minimum distance criteria, V_0 is a constant with unit V, $\mathbf{r}_n = [x_n, y_n, 0]^T$ is the position of the n-th radiating element, N_T is the number of radiating elements in the DRA, $\hat{\boldsymbol{r}}(\theta,\phi) = [\sin\theta\cos\phi, \sin\theta\sin\phi, \cos\theta]^T$ is the unit vector pointing to (θ,ϕ), $(\theta^{(c)}_{b^{(c)}}, \phi^{(c)}_{b^{(c)}})$ is the angular direction of beam $b^{(c)}$ in colour c, k is the free-space wavenumber. Finally, P_0 is the (uniform) power assigned to each beam, and

$$P^{(c)}_{b^{(c)}} = \int_0^{2\pi}\int_0^{\pi/2} \frac{\left|E^{(c)}_{b^{(c)}}(r,\theta,\phi)\right|^2}{2\zeta} r^2 \sin\theta d\theta d\phi, \tag{11}$$

is the surface integral of the Poynting vector of (10) over the spherical surface with radius r. ζ is the free-space impedance.

Fig.5 shows the surface plot of the C/I for the three sublattices in Fig.2. For each u-v point, we assume that the user is served by the closest beam and experiences the interference from all the remaining beams that share the same colour. By comparing Fig.5c with Fig.5a and Fig.5b, we can conclude that the MASCONDS solution provides the best C/I performance among the three solutions. Finally, Fig.6 shows the cumulative distribution function of the C/I for all possible sublattices with $C = 80$. The plots confirm that the MASCONDS solution achieves the largest C/I for the majority of points.

These results are in line with the ones presented in [8], where the antenna is modelled as an ideal circular aperture, and $C = 41$ colours in Ku band are considered.

V. Conclusion

In this letter, we presented a rigorous geometric optimization methodology to tackle the critical problem of mitigating CCI and maximizing C/I in fixed multibeam satellite antennas. The core of our approach involved formally casting the frequency reuse assignment as the problem of finding the sublattice configuration that maximizes the minimum distance ($d_{\min}$) between co-channel beams. We presented the MASCONDS algorithm in [8], which serves as a definitive solution procedure for this challenge. This algorithm leverages the non-redundant properties of the Hermite Normal-Form representation in lattice theory, enabling a systematic and complete enumeration of all possible unique sublattice configurations. Consequently, we are able to guarantee the globally optimal solution for any underlying beam lattice geometry and for an arbitrary reuse factor (C). This capability is vital, as it overcomes the primary limitations of previous, fragmented analytical methods that were restricted to only a few canonical values of C. Finally, we validated the practical efficacy of our method by applying the algorithm-optimized distance approach to a DRA-based GEO communication satellite beam layout using a non-canonical reuse factor. The resulting optimized frequency plan consistently demonstrated superior C/I performance compared to all other feasible sublattice configurations. This work provides system architects with a robust, generalizable, and computationally efficient tool essential for next-generation, high-throughput multibeam system design.

Acknowledgment

This work has been supported by the European Space Agency under contract No. 4000138743/22/NL/GLC/ov.

References

[1] P. Angeletti, R. De Gaudenzi and M. Lisi, "From "Bent Pipes" to "Software Defined Payloads": Evolution and Trends of Satellite Communications Systems," *26th International Communications Satellite Systems Conference* (ICSSC), June 2008

[2] R. De Gaudenzi, P. Angeletti, D. Petrolati and E. Re, "Future technologies for very high throughput satellite systems," *Wiley International Journal of Satellite Communications and Networking*, Vol. 38, No. 2, pp. 141-161, Mar./Apr. 2020, doi: 10.1002/sat.1327

[3] C. Nicolas, V. Enjolras, P. Voisin, C. Boustie, and G. Jestin, "Thales Alenia Space 6th Generation Digital Transparent Processor (DTP6G)-A Multi-mission, Multi-Mode Versatile Product at the Hearth of TELECOM Solutions," *IET Conference Proceedings*, Vol. 2022, No. 29, pp. 25-32, 2022.

[4] J. C. Lafond, E. Vourch, F. Delepaux, P. Lepeltier, P. Bosshard, F. Dubos, C. Feat, C. Labourdette, G. Navarre, and J. M. Bassaler, "Thales Alenia Space multiple beam antennas for telecommunication satellites," *8th European Conference on Antennas and Propagation (EuCAP 2014)*, The Hague, Netherlands, pp. 186-190, 2014

[5] P. Angeletti, and R. De Gaudenzi, "A pragmatic approach to massive MIMO for broadband communication satellites," *IEEE Access*, Vol. 8, pp. 132212-132236, 2020.

[6] V. H. M. Donald, "Advanced mobile phone service: The cellular concept," *The Bell System Technical Journal*, Vol.58, No.1, pp.15-41, 1979.

[7] C. de Almeida, and R. Palazzo, "On the frequency allocation for mobile radio telephone systems," *Proceedings of 6th International Symposium on Personal, Indoor and Mobile Radio Communications*, Toronto (ON), Canada, 1995.

[8] F. Lisi, P. Angeletti, J. F. C. Mota, J. Maurin, H. Legay, and G. Goussetis, "Interference Mitigation in Multibeam Satellite Networks as an Optimal Sublattice Problem," *IEEE Transactions on Communications*, vol. 74, pp. 1940-1951, 2026.

[9] P. Angeletti, "Multiple Beams From Planar Arrays," *IEEE Transactions on Antennas and Propagation*, Vol. 62, No. 4, pp. 1750-1761, Apr. 2014.

[10] P. Q. Nguyen, "Hermite's Constant and Lattice Algorithms," in P. Q. Nguyen, and B. Vallée (Eds), *The LLL algorithm: survey and applications. Information security and cryptography*, Springer, Berlin Heidelberg, pp. 19-69, 2010.

[11] M. Pellet, G. Goussetis, H. Legay, J. Mota, B. Cortazar, and G. Toso, "A new antenna array architecture with hybrid beamforming for broadband satellite communications," *17th European Conference on Antennas and Propagation, EuCAP 2023*, 2023.